

High p_T Charm Photoproduction

G. Abbiendi^a J. M. Butterworth^b, R. Graciani^c

^a Deutsches Elektronen-Synchrotron DESY, Hamburg, Germany

^b Dept. of Physics and Astronomy, University College London, London, UK.

^c Universidad Autonoma de Madrid, Spain.

Abstract: The expected rates for charm-tagged jet photoproduction are evaluated for a number of tagging procedures, and some of the physics potential is discussed. Charm in jets is tagged using D^* 's, μ 's, or tracks from secondary vertices which might be identified in a microvertex detector. We find high expected event rates, leading to the possibility of placing strong constraints on the kinematics of charm production and on the gluon content of the proton and the charm content of the photon.

1 Introduction

At HERA energies interactions between almost real photons (of virtuality $P^2 \approx 0$) and protons can produce jets of high transverse energy (E_T^{jet}). A significant fraction of these jets are expected to arise from charmed quarks. The presence of a 'hard' energy scale means that perturbative QCD calculations of event properties can be confronted with experiment, and hence the data have the potential to test QCD and to constrain the structures of the colliding particles.

At leading order (LO) two processes are responsible for jet production. The photon may interact directly with a parton in the proton or it may first resolve into a hadronic state. In the first case all of the photon's energy participates in the interaction with a parton in the proton. In the second case the photon acts as a source of partons which then scatter off partons in the proton. Examples of charm production in these processes are shown in Fig. 1.

The possibility of experimentally separating samples of direct and resolved photon events was demonstrated in [1], and in [2] a definition of resolved and direct photoproduction was introduced which is both calculable to all orders and measurable. This definition is based upon the variable

$$x_\gamma^{OBS} = \frac{\sum_{jets} E_T^{jet} e^{-\eta^{jet}}}{2yE_e}, \quad (1)$$

where the sum runs over the two jets of highest E_T^{jet} . x_γ^{OBS} is thus the fraction of the photon's energy participating in the production of the two highest E_T^{jet} jets. This variable is used to define cross sections in both data and theoretical calculations. High x_γ^{OBS} events are identified as direct, and low x_γ^{OBS} events as resolved photoproduction.

Charm-tagged jet cross sections have several advantages over untagged jet cross sections. Knowledge of the nature of the outgoing parton reduces the number of contributing subprocesses

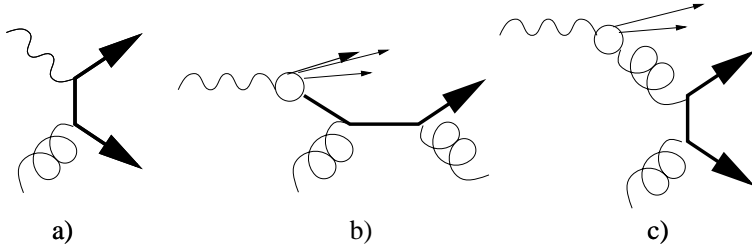


Figure 1: *Examples of charm photoproduction at HERA: a) Direct; photon-gluon fusion, b) Resolved; single excitation of charm in the photon, c) Resolved; gluon-gluon fusion. The charm and anticharm quarks are indicated by the bold lines.*

and thus simplifies calculations and the possible extraction of parton densities, including the charm content of the photon and the gluon content of the proton. Detailed studies of the dynamics of charm production should provide a stringent test of the QCD calculations. In addition, in the case that charm decays are fully reconstructed, the outgoing momenta provide an alternative to calculating the event kinematics from jet momenta, which could provide a useful *model independent* examination of the uncertainties coming from non-perturbative fragmentation effects.

Here we briefly examine the event rates and distributions obtainable with high luminosities using the three charm tagging methods described below. We use the HERWIG 5.8 [3] Monte Carlo simulation, including multiparton interactions [4], along with simple cuts and smearing to mimic the expected gross features of detector effects. We define our starting sample by running the k_T jet algorithm [5] on the final state particles of HERWIG (after the decay of charmed particles) and demanding at least two jets with transverse energy $E_T^{jet} > 6\text{GeV}$ and absolute pseudorapidity $|\eta^{jet}| < 2$. In addition we demand $P^2 < 4\text{GeV}^2$ and $135\text{ GeV} < W_{\gamma p} < 270\text{ GeV}$. This is a kinematic region in which dijet cross sections have already been measured at HERA [2].

According to HERWIG, the total cross section for heavy flavour (b or c) jets in this kinematic region is 1900 pb^{-1} (1000 pb^{-1}) for direct (resolved) photoproduction, using the GRV94 LO proton parton distribution set [6] and the GRV LO photon parton distribution set [7].

There is some evidence [2, 8] that these LO calculations may underestimate the cross section, particularly the resolved cross section, by a factor of around two. On the other hand, the dominant LO subprocess for resolved charm production is predicted to be excitation of charm from the photon. This expectation is not fully reliable: the charm content in the photon is presently overestimated in the available parton distribution sets as they assume only massless quarks. If quark masses are included one would expect the resolved charm cross section to be considerably *smaller* than the number we are quoting here. Its measurement will be an important topic in its own right.

2 Charm tagging methods

2.1 D^* tagging method

Currently, the reconstruction of D^* is the only method used to tag open charm by the HERA experiments in published data [9]. D^* are tagged by reconstructing the D^0 produced in the decay $D^{*\pm} \rightarrow D^0 + \pi^\pm$ and the mass difference $\Delta(M)$ between the D^* and the D^0 .

The overall tagging efficiency for the D^* method is given in table 1, along with the expected number of events after an integrated luminosity of 250 pb^{-1} . For this study we have demanded a D^* with $p_T > 1.5 \text{ GeV}$ and $|\eta| < 2$, and assumed that for these D^* the efficiency of reconstruction is 50%. The decay channels used are $D^* \rightarrow D^0 + \pi \rightarrow (K + \pi) + \pi$ and $D^* \rightarrow D^0 + \pi \rightarrow (K + \pi\pi\pi) + \pi$. A signal/background ratio of around 2 is estimated, although this (as well as the D^* reconstruction efficiency) will depend upon the understanding of the detectors and cuts eventually achieved in the real analysis, which cannot be simulated here.

2.2 μ tagging method

The capability of the μ tagging method has been evaluated using a complete simulation of the ZEUS detector [10] based on the GEANT package [11]. The method itself develops previous work [12] in which a measurement of the total charm photoproduction cross section was obtained in the range $60 < W < 275 \text{ GeV}$. Muons are tagged requiring a match between a track in the ZEUS central tracking detector pointing to the interaction region and a reconstructed segment in the inner muon detectors (which lie about one metre away, outside the uranium calorimeter).

The position and the direction of the reconstructed segment are used to determine the displacements and deflection angles of its projections on two orthogonal planes with respect to the extrapolated track. These quantities are distributed according primarily to the multiple Coulomb scattering within the calorimeter. In comparison the measurement errors are negligible and have not been taken into account. With this approximation and a simple model accounting for the ionization energy loss of the muon through the calorimeter, a χ^2 has been defined from the four variables. The cut on the χ^2 has been chosen to keep 90% of the events with a reconstructed true muon in large Monte Carlo charm samples and checked in selected data samples. The results are contained in table 1.

2.3 Tagging using secondary vertices

If a high resolution microvertex detector is installed close to the interaction region, the tagging of charm by looking for secondary vertices inside jets becomes practical. For this study we have simulated three example methods ('A', very tight cuts and 'B', looser cuts and 'C', very loose cuts) as follows:

- Look at all stable charged tracks which have transverse momentum $p_T(\text{track}) > 500 \text{ MeV}$ and $|\eta(\text{track})| < 2$ and which lie within $\delta R = \sqrt{(\delta\phi)^2 + (\delta\eta)^2} < 1.0$ of the centre of either of the two jets, and
- Assume a (Gaussian) impact parameter resolution for these tracks of $180 \mu\text{m}$ in XY and Z independent of momentum and angle. This corresponds to the design value of the H1 vertex detector [13] for tracks with momentum 500 MeV at 90° .
- Demand at least two tracks which have impact parameters displaced by 3σ (condition A) or one track with an impact parameter displaced by 3σ (condition B) or 2σ (condition C) from the primary vertex.

The results are given in table 1. We note that an enriched sample of b quarks could be obtained by using very tight tagging conditions in a microvertex detector.

Tagging Method	Direct			Resolved		
	Efficiency	N(events)	Sig./Bkgd	Efficiency	N(events)	Sig./Bkgd
D^*	1.4%	6500 (9% b)	≈ 2	0.7%	1700 (4% b)	≈ 1
μ	7.3%	34000 (20% b)	2.0	3.4%	8400 (10% b)	0.3
Vertex A	2.3%	11000 (63% b)	76	1.0%	2500 (34% b)	8
Vertex B	10%	47000 (33% b)	3.4	6.0%	15000 (17% b)	0.5
Vertex C	37%	170000 (17% b)	0.9	32%	79000 (6% b)	0.2

Table 1: *Estimated tagging efficiencies, signal to background ratio and total numbers of expected signal events for various tagging methods after an integrated luminosity of 250 pb^{-1} . The efficiencies given are the ratios of good events which are tagged to all good events. ‘Good events’ are $ep \rightarrow 2$ or more jets with $E_T^{jet} \geq 6 \text{ GeV}$, $|\eta^{jet}| < 2$, for virtualities of the exchanged photon less than 4 GeV^2 in the range $135 \text{ GeV} < W_{\gamma p} < 270 \text{ GeV}$ and where one or more of the outgoing partons from the hard subprocess was a charm or beauty quark. The fraction of the signal events which are from b quarks is also given.*

3 Physics Potential and Conclusions

High luminosity running at HERA will provide large samples of jets containing heavy quarks. These jets can be identified using muons or D^* with efficiencies of a few percent and signal-to-background ratios of around 2. In addition there is the possibility of identifying the electron channel for semi-leptonic decays, which we have not considered here but which could be very effective at these high transverse energies. The presence of a high resolution vertex detector would enormously enrich the tagging possibilities, allowing improved signal-to-noise ratios and/or improved efficiencies (up to around 35%) depending upon the details of the cuts and reconstruction. Combining the tagging methods we have studied here can be expected to give still more flexibility in the experimental selection and cross section measurement.

With the samples of several tens of thousands of charm-tagged jets thus obtainable, jet cross sections can be measured over a wide kinematic range. For the signal events selected by the vertex method B, various distributions are shown in Fig.2. From the x_γ^{OBS} distribution (Fig.2a) we see that the resolved photon component, whilst suppressed relative to the direct component compared to the untagged case [2], is significant. This component is largely due to the charm content in the GRV photon parton distribution set. Measurement of this cross section can be expected to constrain the charm content of the resolved photon and the implementation of the $\gamma \rightarrow c\bar{c}$ splitting in the perturbative evolution. The boson gluon fusion diagram dominates for the high- x_γ^{OBS} range and this cross section is sensitive to the gluon content of the proton in the range $0.003 < x_p^{OBS} < 0.1$, where $x_p^{OBS} = \frac{\sum_{jets} E_T^{jet} e^{\eta^{jet}}}{2E_p}$ is the fraction of the proton’s energy manifest in the two highest E_T^{jet} jets (Fig.2b). The M_{JJ} distribution is shown in Fig.2c, where $M_{JJ} = \sqrt{2E_T^{jet1} E_T^{jet2} [\cosh(\eta^{jet1} - \eta^{jet2}) - \cos(\phi^{jet1} - \phi^{jet2})]}$ is the dijet invariant mass. For $M_{JJ} > 23 \text{ GeV}$ the dijet angular distribution [14] $|\cos\theta^*| = |\tanh(\frac{\eta^{jet1} - \eta^{jet2}}{2})|$ is unbiased by the E_T^{jet} cut. As shown in Fig.2d the angular distributions of high and low x_γ^{OBS} should differ strongly, due to the underlying bosonic (gluon) or fermionic (quark) exchange processes [14]. The measurement of such a distribution should confirm that the dominant charm production process in direct photoproduction was photon-gluon fusion. In addition it will determine whether excitation of charm from the incoming particles or gluon-gluon fusion is the dominant production mechanism in resolved photoproduction.

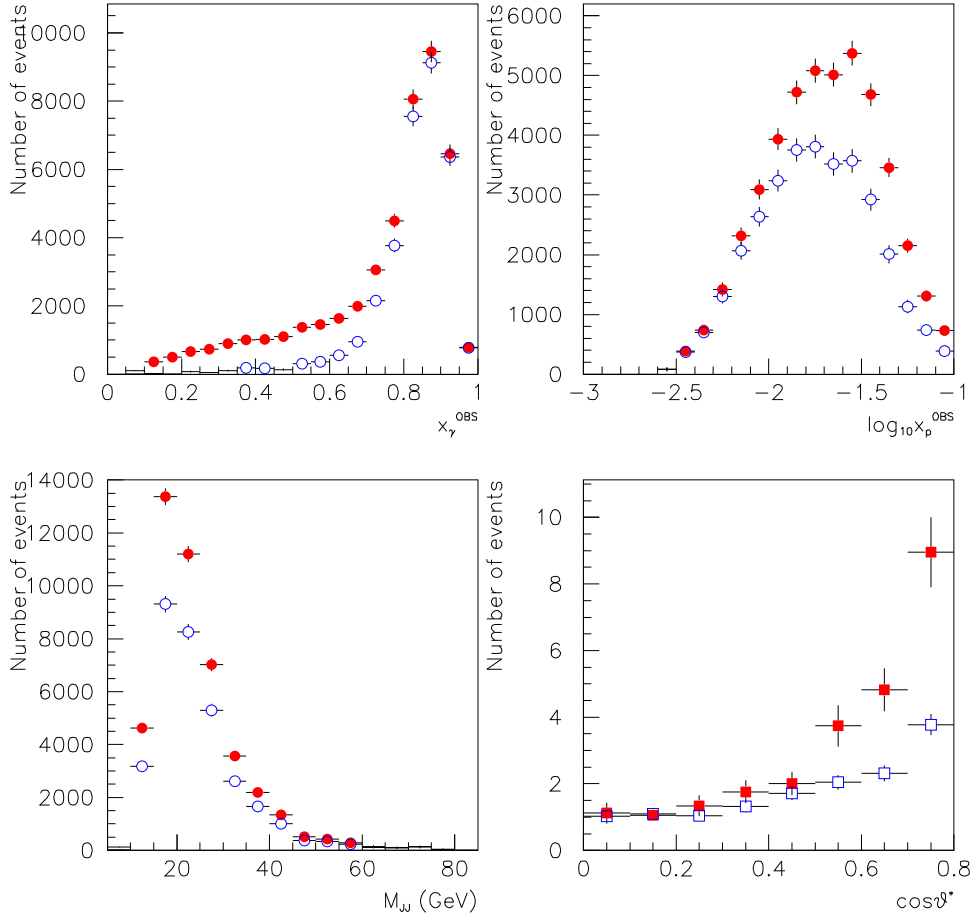


Figure 2: a) x_γ^{OBS} , b) x_p^{OBS} , c) M_{JJ} , and d) $\cos\theta^*$. In a), b) and c), clear circles are the LO direct only, solid dots are the full sample. The normalisation is to 250 pb^{-1} . In d) the solid squares are the $x_\gamma^{OBS} < 0.75$ sample and the clear squares are the $x_\gamma^{OBS} > 0.75$ sample. Both samples are normalised to one at $|\cos\theta^*| = 0$ and the error bars have been scaled to correspond to the statistical uncertainty expected after 250 pb^{-1} .

Acknowledgements

It is a pleasure to thank U. Karshon, D. Pitzl, A. Prinias, S. Limentani and the members and conveners of the working group for discussions and encouragement.

References

- [1] ZEUS Collab., M. Derrick et al., Phys. Lett. B322 (1994) 287.
- [2] ZEUS Collab., M. Derrick et al., Phys. Lett. B348 (1995) 665.
- [3] G. Marchesini et al., Comp. Phys. Comm. 67 (1992) 465.
<http://surya11.cern.ch/users/seymour/herwig/>
- [4] J. M. Butterworth and J. R. Forshaw, J. Phys. G19 (1993) 1657;
J. M. Butterworth, J. R. Forshaw and M. H. Seymour, CERN-TH-95-82, to appear in Zeit. f. Phys. C.
- [5] S. Catani, Yu.L. Dokshitzer, M.H. Seymour and B.R. Webber, Nucl.Phys.B406(1993)187.
S.D. Ellis and D.E. Soper, Phys.Rev.D48(1993)3160.
<http://surya11.cern.ch/users/seymour/ktclus/>
- [6] M. Glück, E. Reya and A. Vogt, Z. Phys. C67 (1995) 433.
- [7] M. Glück, E. Reya and A. Vogt, Phys. Rev. D46 (1992) 1973.
- [8] R. Graciani, for the ZEUS Collab., Rome DIS'96.
U. Karshon, for the ZEUS Collab., QCD'96, Montpellier.
- [9] H1 Collab., C. Adloff et al., DESY 96-138, hep-ex/9607012
H1 Collab., S. Aid et al., DESY 96-055, hep-ex/9604005
ZEUS Collab., M. Derrick et al., Phys. Lett. B 349 (1995) 225.
- [10] ZEUS Collab., The ZEUS Detector, Status Report (1993).
<http://www-zeus.desy.de/bluebook/bluebook.html>
- [11] http://wwwcn.cern.ch/asdoc/geant_html3/geantall.html
- [12] G.Abbiendi, Tesi di Dottorato (1995) Padova University and ZEUS internal note 95-027.
- [13] H1 Collab., Technical Proposal to build Silicon Tracking Detectors for H1, DESY-PRC 92/01.
- [14] ZEUS Collab., M. Derrick et al., DESY 96-094, hep-ex/9605009; to appear in Phys. Lett. B.